Contents lists available at UGC-CARE

International Journal of Pharmaceutical Sciences and Drug Research

[ISSN: 0975-248X; CODEN (USA): IJPSPP]

Available online at www.ijpsdronline.com

Research Article

Screening of Some Hamamelitannin Derivatives against *Staphylococcus aureus*: A Computational Perspective

Kaushik Sarkar, Subhajit Sarkar, Rajesh K. Das*

Department of Chemistry, University of North Bengal, Darjeeling, West Bengal, India.

ARTICLE INFO

Article history:

Received: 07 October, 2022

Revised: 30 October, 2022

Accepted: 03 November, 2022

Published: 30 November, 2022

Keywords:

Hamamelitannin, QSI, molecular docking, molecular dynamics simulation, DFT, ADMET.

DOI:

10.25004/IJPSDR.2022.140623

ABSTRACT

Methicillin-resistant *Staphylococcus aureus* (MRSA) is a common target for inhibiting the quorum sensing biofilm formation. Hamamelitannin (HAM) has a promising activity to combat these biofilm-associated infections and is used as a quorum sensing inhibitor (QSI). Here, we found different tested derivative compounds for designing *S. aureus* biofilm inhibitors by functionalization at various positions of HAM. *In-silico* studies were carried out to find better drug candidature. Out of all, 14 derivatives have satisfied higher binding affinity as well as interactions against three different *S. aureus* target receptors compared to HAM. Density functional theory (DFT), absorption, distribution, metabolism and excretion (ADME), and toxicity analysis are also performed for these compounds. The stability of the protein-ligand complexes is quantified by 30 ns molecular dynamics simulations. From these various studies, 14 ligands will be considered potent inhibitors against *S. aureus* biofilm formation after successfully screening *in-vitro* and *in-vivo* analysis.

Introduction

Nowadays, antimicrobial resistance is increasing rapidly and has thrown a big challenge towards global public health.[1,2] New antimicrobial drugs with more potency are rare in this situation.[3,4] Every year, at least 7 lakh people die from antimicrobial resistance to common bacterial infections.[5] According to a report, it is calculated that the emerging effect of multi-drug resistant infections will drive the lives of approximately 10 million people at risk every year by 2050.[6] The chronic misuse and overuse of antibiotics are the main reason for increasing antibacterial resistance; thus, they are involved in developing highly multidrug-resistant pathogens.[7] Hence, new innovative strategies are required to combat these bacterial infections with the development of new potent antibiotics.[5,8]

Bacteria have been considered as a simple living microorganisms for a long time and it is well known that microbes live in communities.[9] These bacteria form biofilms with complex structure and dynamic systems as they grow on biotic and abiotic surfaces.[10] Generally, biofilms are well-behaving organized communities of microorganisms which are held together by self-made extracellular polymeric substances (organic matrix), and thereby display an altered phenotype compared with free planktonic counterparts.[11] Bacterial biofilms are involved in many medical conditions such as tuberculosis, periodontal disease and respiratory tract infections of the *Staphylococcal* wound.[10] A number of bacteria have been listed by the Centers for Disease Control and Prevention (CDC) which cause serious health problems.[2] Methicillin-resistant *Staphylococcus aureus* (MRSA) is a common example of this type of bacteria. This pathogen may cause a compressive range of clinical infections in humans and animals with higher mortality rates.[12] The rapid emergence of multi-drug resistant capability of this

***Corresponding Author:** Dr. Rajesh K. Das

Address: Department of Chemistry, University of North Bengal, Darjeeling, West Bengal, India.

Email ✉**:** rajeshnbu@gmail.com

Tel.: +91-9434459238

Relevant conflicts of interest/financial disclosures: The authors declare that the research was conducted in the absence of any commercial or financial relationships that could be construed as a potential conflict of interest.

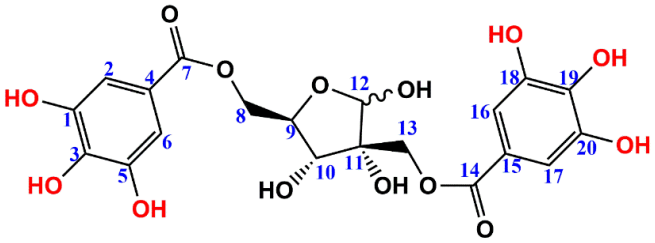

Fig. 1: Structure of hamamelitannin.

pathogen has also been added, becoming an obstruction for public health concern.[13] The human microorganism of this bacteria may even be transformed into various dangerous pathogens and causes wide range of infections including bacteremia, skin or soft tissue infections, endocarditis and toxin related disease.[14] *S. aureus* is a gram-positive bacterium and its virulence factors are controlled by the accessory gene regulator (agr) quorum sensing (QS) system.[10] Under high cell density conditions, this agr system reduces the expression of various colonization factors while increasing the production of many virulence factors. The adherence and invasion of nature are the major key factors of *S. aureus* infections due to the formation ability of biofilms on natural and abiotic surfaces.[15] It is difficult to eradicate the biofilm associated with lethal infections of *S. aureus*; hence, proper treatment has become a challenging aspect with higher cost. The main reason for this is that this type of biofilm protects the cell from both host immune systems as well as from the effects of various chemotherapeutic agents.[16] For a few decades, antibacterial researchers have focused their attention on new drugs that kill bacteria or inhibit their growth by interfering with biofilm formation processes.[10]

QS is a cell to cell communication process in which the population density of bacteria is growing enormously and thus controls the genetically mediated responses. In *S. aureus*, there are two different QS systems to regulate the virulence factor. The first is the agr-mediated system, and the second is the RAP/TRAP system.[17] These two virulence factors alter the gene expression in *S. aureus* by controlling the small signaling molecule RNAIII.[18] The QS signaling process of *S. aureus* agr is controlled by QS inhibitors (QSI) which come out as promising antibiofilm agents to resist biofilm related infections.[13] Several compounds are known to have promising activity to combat these biofilm-associated infections by targeting biofilm matrices of MRSA. Hamamelitannin (2',5-di-O-galloyl-D-hamamelose) (Fig. 1) is one of those promising compounds which have been found to behave as antimicrobial agents.[13] It is a natural product isolated from american witch hazel, *Hamamelis virginiana*. The chemical structure of hamamelitannin (HAM) has important liabilities from the perception of medicinal chemistry. It has a flexible d-hamamelose scaffold in which hydroxyl groups are esterified as gallic acid. The high number of hydroxyl

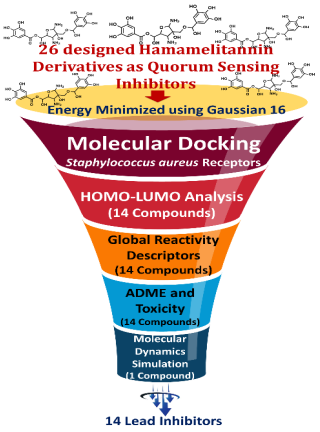

Fig. 2: Schematic representation of this work.

groups makes hamameitannin a highly polar compound with promising bioavailability. Similarly, aromatic hydroxy groups, present in the molecule have helped towards oxidation and glucuronidation.[19] It is regarded to prevent MRSA biofilm-associated infections by blocking the QS system, thereby decreasing its virulence factors[20] and thus used as QSI in *S. aureus*.[21] HAM also interferes with the eDNA release and peptidoglycan thickness through the QS receptor TRAP.[22] HAM has been found as the non-peptide analogue of RNAIII inhibiting protein (RIP) and used as inhibitor *S. aureus* QS of RAP/TRAP (RNAIII activating protein of RAP).[20,23,24] Besides, this natural product has the ability to inhibit biofilm formation and activate the antibiotics against *S. aureus* biofilm *in-vivo* and *in-vitro*.[20,22] Herein, we have designed 14 best derivatives of HAM against the *S. aureus* biofilm by employing computational studies (Fig. 2).

Materials And Methods

Dataset Collection

26 design derivatives along with standard HAM were drawn by using ChemSketch Tool (https://www.acdlabs.com/). The studying compounds having different substituents are shown in Table S1. All explicit hydrogens were added to these compounds and their structures were converted from 2D to 3D format. These compounds were then optimized for studying the density functional theory (DFT).[25,26] The chemical structures of the best derivatives are shown in Fig. 3.

Target Receptor Preparation

In this study, three target receptors i.e., the 3D X-ray crystal structures of *S. aureus* (PDB ID: 4AE5, 4G4K and 2FNP) were downloaded from the Research Collaboratory for Structural Bioinformatics – Protein Data Bank (RCSB – PDB) (http://www.rcsb.org/). All bound waters, ligands and cofactors were removed from these crystal structures prior to docking using Molegro Molecular Viewer (MMV) 2.5.0 suite (CLC Bio, Qiagen Inc.).

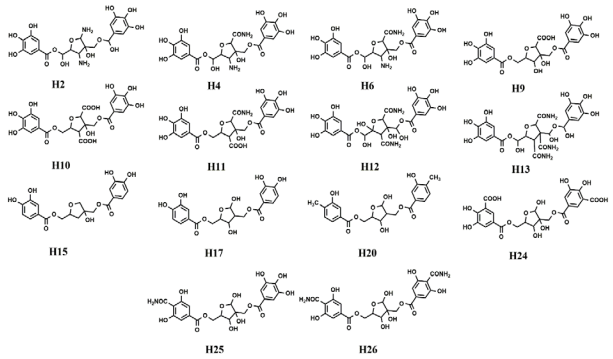

Fig. 3: Chemical structures of best designed HAM derivatives.

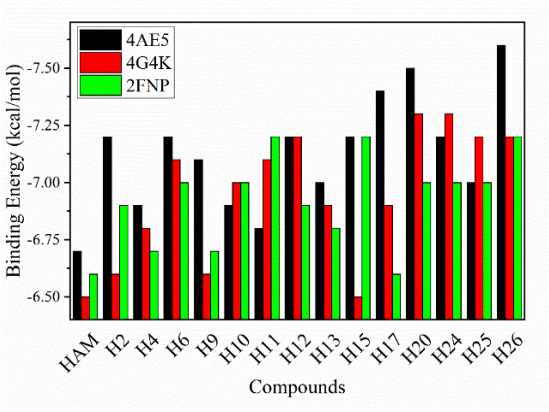

Fig. 4: Compounds having comparable binding energies than hamamelitannin towards target receptor of *S. aureus* with PDB ID: 4AE5 (black), 4G4K (red) and 2FNP (green).

Density Functional Theory (DFT)

Gaussian (G16)[27] software was used to optimize the chemical structure of all compounds. In this study, the DFT model of unrestricted Becke's three parameters exchange potential and Lee-Yang-Parr correlation functional method (UB3LYP) with 6-311++G(d,p) basis set[28,29] was applied for completing the minimized energy search. The optimized chemical structures of the best derivatives are shown in Fig. S1. Energy of the highest occupied molecular orbital (HOMO), lowest unoccupied molecular orbital (LUMO), band gap energy, total minimized energy and dipole moment are shown in Table 1.

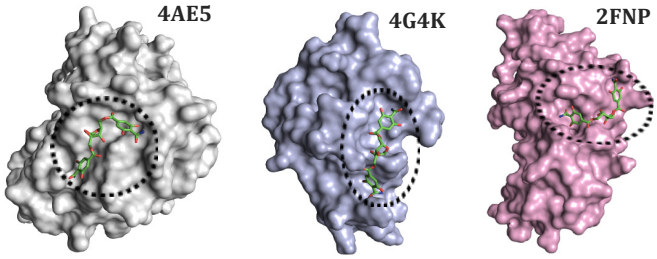

Fig. 5: 3D docking view structure of analogue H26 (green stick) into styphyllococal target receptor (PDB ID: 4AE5, 4G4K and 2FNP).

Molecular Docking Method

Autodock Vina software[30] under Autodock Tools-1.5.6 (ADT) was used to generate the best binding poses of all the ligands. The main reasons for choosing Autodock Vina are that (a) it gives high accuracy in predicting protein-ligand interaction compared to Autodock 4.2, (b) requires shorter running time because of its multiple core processors and (c) finds more accuracy for ligand processing having more than 20 rotatable bonds.[31] The receptor molecules were prepared by adding all polar hydrogen with no bond order, using the graphical user interface of ADT. All the ligands were also prepared as PDB format from all the optimized Gaussian output to assist rigid docking, using the Avogadro suite. Active torsions have been assigned

Table 1: Calculated energy values of hamamelitannin and its derivatives using UB3LYP/6-311++G(d,p) basis set

Compound	E_{HOMO} *(eV)*	E_{LUMO} *(eV)*	*Band gap* (ΔE_{HL}) *(eV)*	$E_{TOTAL}x10^{-4}$ *(eV)*	*Dipole moment (Debye)*
Hamamelitannin	-6.09	-1.85	4.25	-4.97	7.84
H2	-6.26	-1.42	4.83	-5.07	6.53
H4	-3.75	-1.43	2.31	-5.38	6.08
H6	-6.00	-2.02	3.98	-5.69	2.37
H9	-6.39	-1.82	4.57	-5.28	1.81
H10	-6.55	-1.82	4.73	-5.59	7.20
H11	-6.61	-1.71	4.89	-5.54	4.86
H12	-6.32	-2.08	4.24	-6.10	4.33
H13	-6.63	-1.98	4.65	-6.15	3.32
H15	-6.31	-1.96	4.35	-4.15	8.46
H17	-6.25	-1.75	4.50	-4.36	8.36
H20	-6.47	-1.62	4.86	-4.16	4.12
H24	-6.93	-2.20	4.73	-5.59	5.88
H25	-6.44	-2.14	4.30	-5.23	10.03
H26	-6.62	-2.32	4.30	-5.48	6.90

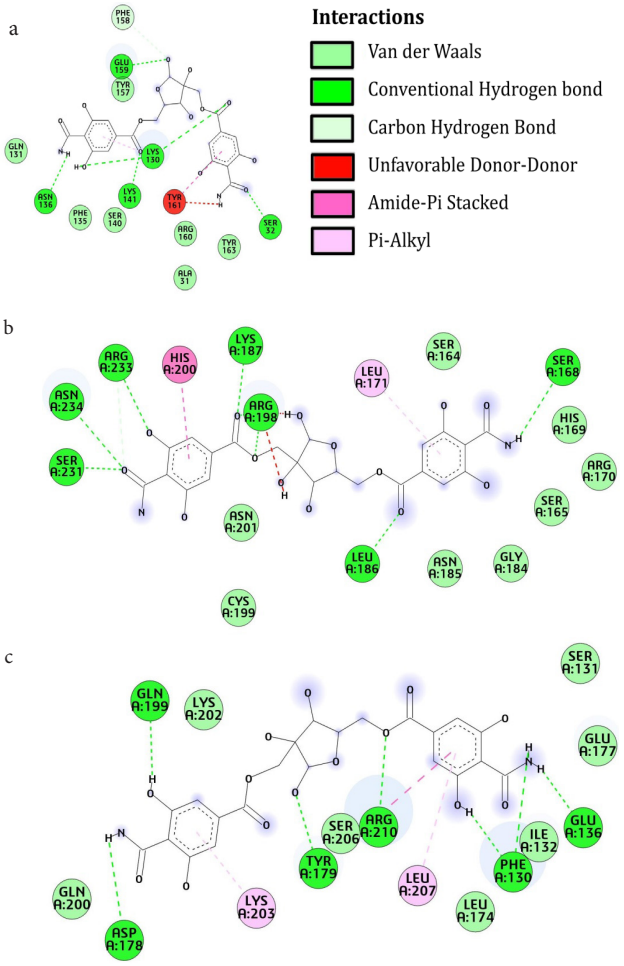

Fig. 6: 2D docking view structure of analogue H26 into *S. aureus* receptor targets with PDB ID (a) 4AE5, (b) 4G4K and (c) 2FNP.

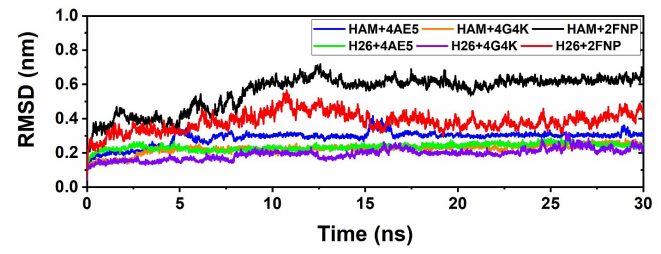

Fig. 7: RMSD plot of protein-ligand complexes with PDB ID 4AE5, 4G4K, 2FNP.

to the maximum number of atoms. Kollman charges were applied to the protein. The ligand and protein molecules were converted to their proper readable format (pdbqt). The grid box size was fixed at dimensions 90×90×90Å, 84×84×84Å and 95×95×95Å for 4AE5, 4G4K and 2FNP receptors, respectively. Similarly, the grid box's x, y and z coordinates were fixed at 5.747, 33.294 & 13.955 for 4AE5; 33.642, 37.868 & 42.418 for 4G4K; 8.942, 3.556 & 13.125 for 2FNP target with an overall spacing of 0.375 Å. In general, all other docking parameters were kept to default values. The best docked models, with higher negative binding energies, were considered for further studies. The resulted pdbqt formats of docked complexes were converted to pdb format using python script (PMV 1.5.6).[32] The output files (protein-ligand complex) were further analyzed using Discovery Studio Visualizer (v20.1.0.19295).

ADMET Properties

PreADMET (http://preadmet.bmdrc.org/) and swissADME (http://www.swissadme.ch/) web server were used to analyze ADME profiles (Absorption, Distribution,

Table 2: Lipinski rule of five data for various compounds

Compound	*MW*[†]	*log$P_{o/w}$ (XLOGP3)*	*Rotatable bonds*	*H-bond acceptors*	*H-bond donors*	*Lipinski violations*
Hamamelitannin	484.36	-1.05	8	14	9	2
H2	500.41	-2.29	8	15	11	3
H4	526.40	-1.23	9	15	10	3
H6	554.41	-2.02	10	15	10	3
H9	512.37	-0.35	9	15	9	3
H10	540.38	-0.20	10	16	9	3
H11	539.40	-0.85	10	15	9	3
H12	586.41	-2.76	10	17	12	3
H13	597.44	-3.59	11	16	11	3
H15	420.37	1.15	8	10	5	0
H17	436.37	0.71	8	11	6	2
H20	432.42	2.15	8	9	4	0
H24	540.38	-0.19	10	16	9	3
H25	511.39	-0.72	9	14	9	3
H26	538.42	-0.39	10	14	9	3

[†]Molecular weight

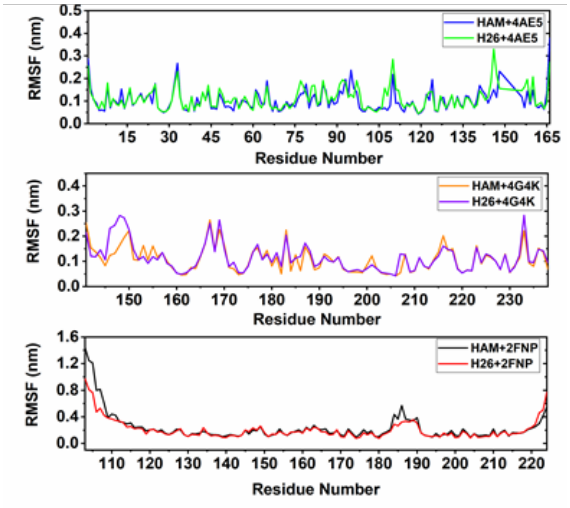

Fig. 8: RMSF of all amino acids of the protein 4AE5, 4G4K, 2FNP, complexes with different ligands.

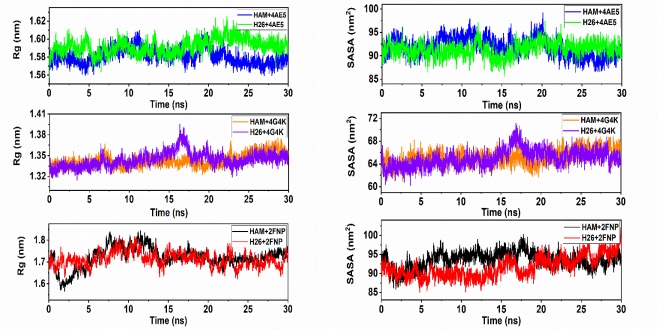

Fig. 9: Rg and SASA plots of the protein-ligand complexes.

Metabolism, and Excretion). The various physical descriptors, namely H-bond donors and acceptors, topological polar surface area (TPSA), number of rotatable bonds etc., for all compounds were predicted by using swissADME. Further, toxicological profiling of all ligands was done using OSIRIS property explorer (http://www.organic-chemistry.org/prog/peo/). The overall toxicity of most active derivative compounds was predicted by the OSIRIS program as it indicates fragment based characteristics responsible for mutagenic, tumorigenic, irritant, and reproductive effects.

Molecular Dynamics (MD) Simulation

MD simulation study using GROMACS 5.1.1 (http://www.gromacs.org/Downloads) was performed with the minimum energy conformers of standard HAM and best designed ligand H26, obtained after docking with three receptors (PDB ID: 4AE5, 4G4K and 2FNP). Topology of protein was constructed in pdb2gmx using CHARMM36-jul2021 force-field[33] and TIP3P solvation model,[34] while ligand topology was generated using CHARMM General Force Field server (CGenFF).[35,36] In this study, we used cubic periodic box setting a minimal distance of 1.0 nm between the protein and the edge of the box. All the protein moieties were neutralized by adding adequate number of ions. Using steepest descent algorithm and conjugate gradient protocol, energy minimization was performed until the maximum force of at least 10 kJ mol^{-1} nm^{-1}. Isochoric-isothermal (NVT) and isothermal-isobaric (NPT) ensembles were applied on the system for 100 ps for equilibration at 300K by keeping 2-fs time step and 1.2 nm electrostatic and van der Waal cut-offs. Particle mesh Ewald (PME)[37] method was used for long range electrostatic interaction calculations. Finally, 30 ns MD simulation was subjected to the equilibrated ensembles with the same cut-offs. Various geometrical properties of the systems such as root mean square deviation (RMSD), root mean square fluctuation (RMSF), solvent-accessible surface area (SASA) and radius of gyration were determined using gmx rmsd, gmx rmsf, gmx sasa and gmx gyrate programs. The graphs were plotted using origin tool.

Results

Docking studies of HAM with three target proteins of PDB ID 4AE5, 4G4K and 2FNP have shown the binding energy value of -6.7, -6.5 and -6.6 kcal/mol respectively. Here, the calculated binding affinities of the selected 14 compounds have shown higher value than HAM (Table. S2). Fig. 4 has displayed the comparison of these calculated binding energies. These 14 compounds are also examined in terms of DFT and other pharmacokinetics studies. It can be found as suitable for Lipinski,s rule of five[38] shown in Table 2. On the other side, Table 3 represents the oral bioavailability and permeability of these compounds. The physical parameters derived from these compounds, such as ionization potential (I), electron affinity (A), global hardness (η), softness (S), chemical potential (μ), electronegativity (σ), and electrophilicity (ω), also played an important role in determining their activity (Table S3). Table S4 has shown the drug score and drug-likeness values for these ligands. The lack of a promising drug is dependent on its toxicity profile. Using OSIRIS Property Explorer, toxicity predictions are made for all 14 derived compounds (Table S4). The OSIRIS toxicity characteristics are presented as color codes, with green denoting low toxicity, yellow expressing medium toxicity, and red indicating high toxicity.

Discussion

It has been reported that the combined effect of HAM with vancomycin has a significant ability to kill biofilm cells *in-vitro*. HAM has been used as a scaffold for developing novel vancomycin potentiators against *S. aureus* biofilms.[22] Since there is no structural knowledge about the inhibitor–target interaction, much of the research has focused on iterative bioactivity driven analogue design, which uses synthetic and medicinal chemistry to find compounds with higher activity and provide information about target interactions. Vermote *et al.* synthesized a

Table 3: ADME parameters for best hamamelitannin derivatives

Compound	*MDDR[a] like rule*	*TPSA[b]*	*HIA[c] %*	*BBB[d] permeant*	*PPB[e] %*	*Skin Permeability*	*Bioavailability Score*
Hamamelitannin	Drug like	243.90	2.63	No	81.71	-4.19	0.17
H2	Drug like	278.87	0.64	No	39.65	-4.56	0.17
H4	Drug like	292.78	0.66	No	57.48	-4.40	0.17
H6	Drug like	309.85	0.41	No	72.71	-4.11	0.17
H9	Drug like	260.97	1.77	No	78.47	-3.99	0.11
H10	Drug like	278.04	1.15	No	78.71	-3.69	0.11
H11	Drug like	283.83	1.07	No	75.76	-3.98	0.11
H12	Drug like	350.31	0.00	No	60.07	-3.67	0.17
H13	Drug like	352.94	0.00	No	55.65	-4.10	0.17
H15	Drug like	162.98	46.98	No	80.65	-3.81	0.55
H17	Drug like	183.21	25.11	No	76.76	-4.26	0.17
H20	Drug like	142.75	75.97	No	82.85	-3.92	0.55
H24	Drug like	278.04	1.16	No	55.01	-4.07	0.11
H25	Drug like	266.76	1.74	No	68.64	-4.37	0.17
H26	Drug like	289.62	1.06	No	58.56	-4.44	0.17

[a]Molecular Detection of Drug Resistance
[b]Topological polar surface area
[c]Human intestinal absorption
[d]Blood brain barrier
[e]Plasma protein binding

series of HAM analogs on the basis of three modifications at the HAM scaffold: isosteric replacement of the ester groups, systematic modification or elimination of the aromatic hydroxyl groups, and removal of the anomeric hydroxyl group to replace the hamamelose core with a tetrahydro furan ring.[19] The effect of HAM analogs on *S. aureus* biofilm susceptibility reveals that ester substitution with an amide moiety, elimination of the anomeric hydroxyl, and finally removal of phenolic groups are all well tolerated. To better understand the HAM scaffold, a library of 21 derivatives was developed, consisting of analogues with various substituents at the ortho position of the 5-phenyl ring and analogues with alternative nitrogen-based linkers in place of the 5-amido group. The use of a sulfonamide group in place of the 5-amide linker was also found to be effective.[10] In this study, we have designed the various derivatives by incorporating active functional groups in the benzene and the five-member ring similar to Skogman *et al.*[39] which used flavone backbone with varying substituents to develop better QSIs.

Molecular Docking Studies

The Autodock Vina program was used to calculate the best binding conformation of each molecule into the binding sites of *S. aureus* receptors. Table S2 summarizes the best docking energy results of these compounds. We got satisfactory docking result, when the substitution jobs were done by hydroxyl, amine, amide, and carboxylic acid groups.[40] The docking results indicate that 14 derived compounds have shown better binding energy results than standard HAM molecules (Fig. 4). 3D and 2D docking interaction of the best compound (H26) is shown in Fig. 5 and 6. Test 4 derivatives have displayed the highest binding energies (<-7 kcal/mol), whereas the other 10, have higher or relatively higher value than HAM in the case of all three receptors.

Mono substituted amine group in d-hamamelose scaffold of H1 (C-12 position) with two hydroxyl groups at C-8 and C-14 positions have not shown satisfactory docking value. Further introduction of one more amine group at the C-10 position of d-hamamelose scaffold (H2) has shown better binding interaction than the previous one. One more substitution of –OH group by $–NH_2$ group, found in H3 at C-11 position of d-hamamelose scaffold has not produced satisfactory binding value due to the presence of steric hindrance. Substitution of one amine by amide (C-12) in H2 with C-14 position remains the same as HAM has shown approximately the same binding energy compared to standard compound. Further substitution of one amine by amide at C-10 position of H5 (results H6) has also satisfied better binding capacity with higher binding energy, compared to the previous one. Similarly, one more substitution of amine by amide found in H7 at C-11 position has not generated satisfactory binding affinity due to the presence of strong vander waals interaction, steric hindrance of three bulkier amide groups found in d-hamamelose scaffold. Substitution of two amines by amides (C-10 and C-12 positions) and hydrogen by hydroxyl

at C-13 in H2 with C-14 position remains the same as HAM has given a decreasing tendency of binding energy found in H8, compared to H2. Mono substituted polar carboxylic acid group found in H9 of d-hamamelose scaffold at C-12 position has shown better docking result. Further introduction of one more acid group, found in H10, has multiplied the binding capability by increasing the polarity of the compound. Substitution of –COOH by amide at C-12 position of H10, found in H11, has also shown satisfying binding ability. On the other hand, elimination of one highly polar –OH group from both phenyl rings and all the same groups from the d-hamamelose scaffold of HAM, found in H14 have significantly decreased the binding activity. However, introducing one or two –OH groups in the d-hamamelose scaffold has shown better binding activity for compounds H15 and H17, but decreased binding energy for compounds H16.

Incorporation of two non-polar $–CH_3$ groups instead of –OH into the phenyl side chain at C-3 and C-19 positions and two hydrogen atoms at C-5 and C-20 instead of polar–OH, resulting in H20, has given higher binding energy with higher stability. But incorporation of two$–CH_3$ groups at C-1 and C-18 positions instead of two–OH groups, found H21, has surprisingly given lower binding energy with least stability. Elimination of all polar–OH groups from HAM (found in H23) has shown the lowest binding activity among all derivatives due to the decreasing order of their interaction tendency. Similarly, incorporation of two highly polar –COOH groups instead of –OH at the phenyl side chain of HAM, resulting in H24, has given higher binding energy. But incorporation of one $–CONH_2$ group instead of –OH at the C-3 position of the benzene ring of HAM, found H25, has also shown similar binding interactions into the active site of *S. aureus* target. Further substitution of second $–CONH_2$ group into another phenyl ring of H25 (found in H26) has shown the highest binding activity. In all of these cases, larger electrostatic, vander Waals, H-bonds and solvation interactions have played the crucial role in increasing binding activity into the binding site with much better value of binding energies.

Frontier Molecular Orbitals (FMOs)

HOMO-LUMO Analysis

The stability of a compound in a chemical sense is mostly dependent on FMOs theory which can explain it on the basis of HOMO (highest occupied molecular orbital) and LUMO (lowest unoccupied molecular orbital) energies.[41] Here, unrestricted B3LYP/6-311++G(d,p) DFT method was applied to calculate the HOMO and LUMO energies of each compound. HOMO has an electron-donating tendency to act as a nucleophile. On the other side, LUMO has an electron-accepting tendency to act as an electrophile.[42] The band gap between HOMO and LUMO (ΔE_{HL}) gives ideas about chemical reactivity and kinetic stability of a molecule. Molecule with large ΔEHL is considered as a hard species and less polarizable (Table 1). Similarly, molecule with small ΔE_{HL} has high chemical reactivity as well as polarizability and considered as soft.[43,44] On the other hand, higher dipole moment value of a molecule indicates better tendency to participate in strong intermolecular interaction. Chemical reactivity of a molecule depends on chemical softness and the reverse is found in the case of hardness.[45] In this study, three derived molecules (H4, H6 and H12) have shown lower ΔE_{HL} compared to standard HAM (4.25 eV), of which H4 is the lowest (2.31 eV) (Table 1). Hence, H4 is considered as a soft molecule with highly polarizable as well as highly reactive (chemically) species. Besides, other remaining molecules also have satisfactory ΔE_{HL} values as compared to HAM which are between 4.25 to 4.9 eV. It is also found that H15, H17 and H25 have satisfied greater dipole moment values as compared to HAM (7.84 D) and thus have a better tendency to participate in strong intermolecular interactions. In this case, H25, which contains the highest dipole moment value of 10.03 D, has a higher tendency to participate in strong intermolecular interaction.

Global Reactivity Descriptors

Global reactivity descriptors have been used to understand a drug molecule's pharmacological and eco-toxicological properties. These DFT based parameters can easily explain the reactivity of a molecule by calculating the chemical potential, global hardness, softness and electrophilicity index. Using HOMO and LUMO energies, the ionization potential (I), electron affinity (A), chemical potential (μ), global hardness (η), global softness (S), electronegativity (σ) and electrophilicity index (ω) can be expressed as:

$$I = -E_{HOMO} \quad A = -E_{LUMO} \quad \mu = {}^1/_2\,(E_{LUMO} + E_{HOMO}) \quad \eta = {}^1/_2\,(E_{LUMO} - E_{HOMO})$$

$$S = {}^1/_{\eta} \qquad \sigma = -\mu \qquad \omega = \frac{\mu^2}{2\eta}$$

Global hardness parameter has determined the chemical stability of a system by measuring the resistivity of its changing electronic charge distribution.[46-48] ω was first introduced by Parr and has determined the electron-accepting capacity of a species.[45] The large chemical softness values ($S \geq 0.47eV^{-1}$) of H6, H12, H25 and H26 with low chemical potential (μ <-3.97eV) may lead to these compounds as soft with higher polarizablility than other of this series. On the other hand, high electronegativity (σ >4.09eV) and elecrophilicity index (ω >4.36eV) of H6, H9, H10, H12, H13, H15, H20, H24, H25 and H26 have higher electron withdrawing capacity to act like electrophile.

ADME and Toxicity Analysis

In-silico drug like properties, bioactive scores were predicted here to select the best drug candidates using OSIRIS suite, preADMET and swissADME online property toolkit. Mutagonic, tumorigenic, irritant, reproductive index and drug-like, drug score values were visualized from OSIRIS and swissADME predicts such valuable parameters like Molecular weight (MW), $logP_{o/w}$, TPSA, number of rotat-

able bonds, number of hydrogen bond acceptors & donors and violations parameters from Lipniski's rule. From this web server, we have also predicted all tested compounds' blood brain barrier (BBB) permeability and bioavailability score. Permeability across the cell membrane of a molecule depends on $logP_{o/w}$. TPSA predicts the tendency of H-bond interactions of a species. The number of rotatable bonds denotes the flexibility of a species. Molecular properties and structural features, irrespective of known drugs, are checked on the basis of drug-likeness data of molecules.[48] The excellent results have shown the probability of these compounds as future QSIs.

Compounds with number of violation ≤1 have better bioavailability and here only two derived compounds (H15 and H20) have qualified by applying Lipinski's rule of five of bioavailable drug. Compounds with H-bond donors ≤ 5 have higher probability to solubile in cellular membranes.[49] In this case, all the compounds (except H15 and H20) are deviated from this rule. Similarly, these two molecules (H15 and H20) have also shown H-bond acceptors ≤ 10 to pass Lipniski's rule. One interesting notation is that the parent HAM has crossed the H-bond accepting and donating capacity and displayed Lipinski violation of 2 due to the presence of a higher number of polar hydroxyl groups. Similarly, all the remaining derivatives have also crossed the same barrier of violation ≥2.

The ADME pharmacokinetic property denotes absorption, distribution, metabolism and excretion phenomena for a drug molecule.[50] Here, ADME profiles of most of these derived compounds have shown satisfactory result. Three compounds namely, H15 (46.98%), H17 (25.11) and H20 (75.97%) have given acceptable values for human intestinal absorption (HIA) compared to standard HAM. *In-vivo* blood brain barrier (BBB) has indicated permeable tendency into the central nervous system (CNS), implying a lower likelihood of cross-over for these molecules. Plasma protein binding data PPB >80% (H15; 80.65% and H20; 82.85%), have shown strong binding tendency and skin permeability. From these all useful parameters, it may conclude that most of these designed compounds have better drug likeness behavior or acceptable ADME properties.

MD Simulation Analysis

The best protein-ligand docked complexes of *S. aureus* target with three different receptors (PDB ID: 4AE5, 4G4K and 2FNP) along with one best inhibitor (H26) were simulated for understanding the structural deviations in the dynamic environment for the time scale of 30 ns. Each inhibitor along with their complexes was recorded for root mean square deviation (RMSD) from its initial position and the calculated values were plotted in Fig. 7. It has been found that RMSD of the complexes have shown satisfactory stability in dynamic conditions. In case of 4AE5 and 2FNP receptors, the receptor-H26 and standard receptor-HAM complexes have shown similar RMSD patterns up to 4 ns. But after this time period, the RMSD lines of the reference compound have increased and shown parallel lines with respect to X-axis. Similarly, for 4G4K receptor, both the RMSD lines have shown a similar parallel pattern (about 0.1 nm) up to 2.5 ns. After that, the RMSD line of the reference complex is slightly increased again than that of designed one and almost coincide at 30 ns. In all these cases, all the RMSD lines have shown parallel pattern with time axis. Hence, the protein-ligand complex of designed H26 has satisfied higher stability than that of the reference complex due to lower RMSD pattern.

In Fig. 8**,** we have shown the root mean square fluctuation (RMSF) of both the two complexes in case of these three receptors, which actually measures the deviation of each amino acid of the used protein over the time interval of 30 ns. The overall results have shown that RMSF values of all the amino acids of the proteins docked with the best inhibitor H26 do not change considerably as compared to standard HAM. Fig. 9 illustrates the radius of gyration (Rg) and solvent accessible surface area (SASA) plots. Rg and SASA have determined the compactness and fluctuation of any system. Here, both the protein-ligand complexes in case of these three receptors correspond to almost similar Rg and SASA values, revealing similar compactness as well as fluctuation of the docked structures.

The present study describes the computational design of small molecule QSIs (derivatives of HAM) against *S. aureus* biofilm formation. Molecular docking analysis, MD simulation, quantum mechanical examination, drug-likeness and toxicity prediction were used in this systematic investigation. Out of 26 derivatives, 14 ligands (H2, H4, H6, H9, H10, H11, H12, H13, H15, H17, H20, H24, H25 and H26**)** have shown significant binding affinity compared to HAM and all these ligands come to light as effective inhibitors against *S. aureus* receptor. Finally, quantum mechanical study confirm the chemical reactivity, while molecular docking, ADME-toxicity parameters, and MD simulations study support it's efficient drug-like behaviour, and higher promising binding affinities also against *S. aureus*. It may conclude from these results that these 14 ligands are effective inhibitors of *S. aureus* biofilm formation after successfully qualifying of *in-vitro* and *in-vivo* analysis.

Acknowledgement

The Authors are thankful to UGC, New Delhi for fellowship and the High Performance Computing (HPC) cluster of University of North Bengal for computational facility, Department of Chemistry for support and also thankful to all Indian people for giving golden opportunity to do this wonderful research.

References

1. Ventola CL. The antibiotic resistance crisis: part 1: causes and threats. P T. 2015;40(4):277-83.

2. Bouton J, Van Hecke K, Rasooly R, Van Calenbergh S. Synthesis of pyrrolidine-based hamamelitannin analogues as quorum sensing inhibitors in Staphylococcus aureus. Beilstein J Org Chem. 2018;14:2822-8.
3. Payne DJ, Gwynn MN, Holmes DJ, Pompliano DL. Drugs for bad bugs: confronting the challenges of antibacterial discovery. Nat Rev Drug Discov. 2007;6(1):29-40.
4. Powers JH. Antimicrobial drug development--the past, the present, and the future. Clin Microbiol Infect. 2004;4:23-31.
5. Czaplewski L, Bax R, Clokie M, Dawson M, Fairhead H, Fischetti VA, et al. Alternatives to antibiotics-a pipeline portfolio review. Lancet Infect Dis. 2016;16(2):239-51.
6. Vermote A, Brackman G, Risseeuw MDP, Coenye T, Van Calenbergh S. Novel hamamelitannin analogues for the treatment of biofilm related MRSA infections-A scaffold hopping approach. Eur J Med Chem. 2017;127:757-70.
7. Lowy FD. Antimicrobial resistance: the example of Staphylococcus aureus. J Clin Invest. 2003;111(9):1265-73.
8. Brown ED, Wright GD. Antibacterial drug discovery in the resistance era. Nature. 2016;529(7586):336-43.
9. Costerton JW, Geesey GG, Cheng KJ. How bacteria stick. Sci Am. 1978;238(1):86-95.
10. Vermote A, Brackman G, Risseeuw MDP, Coenye T, Van Calenbergh S. Design, synthesis and biological evaluation of novel hamamelitannin analogues as potentiators for vancomycin in the treatment of biofilm related Staphylococcus aureus infections. Bioorg Med Chem. 2016;24(19):4563-75.
11. Lewis K. Multidrug tolerance of biofilms and persister cells. Curr Top Microbiol Immunol. 2008;322:107-31.
12. Tong SY, Davis JS, Eichenberger E, Holland TL, Fowler VG, Jr. Staphylococcus aureus infections: epidemiology, pathophysiology, clinical manifestations, and management. Clin Microbiol Rev. 2015;28(3):603-61.
13. Abd El-Hamid MI, ES YE-N, T MK, Hegazy WAH, Mosbah RA, Nassar MS, et al. Promising Antibiofilm Agents: Recent Breakthrough against Biofilm Producing Methicillin-Resistant Staphylococcus aureus. Antibiotics. 2020;9(10).
14. Lowy FD. Staphylococcus aureus infections. N Engl J Med. 1998;339(8):520-32.
15. Laverty G, Gorman SP, Gilmore BF. Biomolecular mechanisms of staphylococcal biofilm formation. Future Microbiol. 2013;8(4): 509-24.
16. Van Acker H, Van Dijck P, Coenye T. Molecular mechanisms of antimicrobial tolerance and resistance in bacterial and fungal biofilms. Trends Microbiol. 2014;22(6):326-33.
17. Brackman G, Coenye T. Inhibition of Quorum Sensing in Staphylococcus spp. Curr Pharm Des. 2015;21(16):2101-8.
18. Sully EK, Malachowa N, Elmore BO, Alexander SM, Femling JK, Gray BM, et al. Selective chemical inhibition of agr quorum sensing in Staphylococcus aureus promotes host defense with minimal impact on resistance. PLoS Pathog. 2014;10(6).
19. Vermote A, Brackman G, Risseeuw MD, Vanhoutte B, Cos P, Van Hecke K, et al. Hamamelitannin Analogues that Modulate Quorum Sensing as Potentiators of Antibiotics against Staphylococcus aureus. Angew Chem Int Ed Engl. 2016;55(22):6551-5.
20. Kiran MD, Adikesavan NV, Cirioni O, Giacometti A, Silvestri C, Scalise G, et al. Discovery of a quorum-sensing inhibitor of drug-resistant staphylococcal infections by structure-based virtual screening. Mol Pharmacol. 2008;73(5):1578-86.
21. Vermote A, Brackman G, Risseeuw MD, Cappoen D, Cos P, Coenye T, et al. Novel Potentiators for Vancomycin in the Treatment of Biofilm-Related MRSA Infections via a Mix and Match Approach. ACS Med Chem Lett. 2016;8(1):38-42.
22. Brackman G, Breyne K, De Rycke R, Vermote A, Van Nieuwerburgh F, Meyer E, et al. The Quorum Sensing Inhibitor Hamamelitannin Increases Antibiotic Susceptibility of Staphylococcus aureus Biofilms by Affecting Peptidoglycan Biosynthesis and eDNA Release. Sci Rep. 2016;6(20321).
23. Giacometti A, Cirioni O, Gov Y, Ghiselli R, Del Prete MS, Mocchegiani F, et al. RNA III inhibiting peptide inhibits in vivo biofilm formation by drug-resistant Staphylococcus aureus. Antimicrob Agents Chemother. 2003;47(6):1979-83.
24. Balaban N, Cirioni O, Giacometti A, Ghiselli R, Braunstein JB, Silvestri C, et al. Treatment of Staphylococcus aureus biofilm infection by the quorum-sensing inhibitor RIP. Antimicrob Agents Chemother. 2007;51(6):2226-9.
25. Parr RG. W. Yang Density functional theory of atoms and molecules. O xford University Press. 1989;1:989.
26. Dreizler RM, da Providência J. Density functional methods in physics: Springer Science & Business Media; 2013.
27. Frisch MJ, Trucks GW, Schlegel HB, Scuseria GE, Robb MA, Cheeseman JR, et al. Gaussian 16 Rev. C.01. Wallingford, CT2016.
28. Stephens PJ, Devlin FJ, Chabalowski CF, Frisch MJ. Ab initio calculation of vibrational absorption and circular dichroism spectra using density functional force fields. The Journal of physical chemistry. 1994;98(45):11623-7.
29. Lee C, Yang W, Parr RG. Development of the Colle-Salvetti correlation-energy formula into a functional of the electron density. Physical review B. 1988;37(2):785.
30. Trott O, Olson AJ. AutoDock Vina: improving the speed and accuracy of docking with a new scoring function, efficient optimization, and multithreading. Journal of computational chemistry. 2010;31(2):455-61.
31. Narkhede RR, Cheke RS, Ambhore JP, D SHİNDE S. The molecular docking study of potential drug candidates showing anti-COVID-19 activity by exploring of therapeutic targets of SARS-CoV-2. Eurasian Journal of Medicine and Oncology. 2020;4(3):185-95.
32. Sanner MF. Python: a programming language for software integration and development. J Mol Graph Model. 1999;17(1):57-61.
33. Lee S, Tran A, Allsopp M, Lim JB, Hénin J, Klauda JB. CHARMM36 united atom chain model for lipids and surfactants. The journal of physical chemistry B. 2014;118(2):547-56.
34. Boonstra S, Onck PR, van der Giessen E. CHARMM TIP3P water model suppresses peptide folding by solvating the unfolded state. The journal of physical chemistry B. 2016;120(15):3692-8.
35. Vanommeslaeghe K, Hatcher E, Acharya C, Kundu S, Zhong S, Shim J, et al. CHARMM general force field: A force field for drug-like molecules compatible with the CHARMM all-atom additive biological force fields. 2010;31(4):671-90.
36. Vanommeslaeghe K, MacKerell Jr AD. Automation of the CHARMM General Force Field (CGenFF) I: bond perception and atom typing. Journal of chemical information and modeling. 2012;52(12):3144-54.
37. Abraham MJ, Gready JE. Optimization of parameters for molecular dynamics simulation using smooth particle-mesh Ewald in GROMACS 4.5. Journal of computational chemistry. 2011;32(9):2031-40.
38. Rastogi S, Rastogi P, Mendiratta N. Bioinformatics Methods And Applications: Genomics Proteomics And Drug Discovery 3Rd Ed: PHI Learning Pvt. Ltd.; 2008.
39. Skogman ME, Kanerva S, Manner S, Vuorela PM, Fallarero A. Flavones as Quorum Sensing Inhibitors Identified by a Newly Optimized Screening Platform Using Chromobacterium violaceum as Reporter Bacteria. Molecules. 2016;21(9).
40. Sarkar K, Sarkar S, Das RK. Screening of drug efficacy of Rosmarinic Acid derivatives as Aurora kinase inhibitors by computer aided drug design method. Curr Comput Aided Drug Des. 2020;3(10):1573409 916666200703170045.
41. Umar Y, Abdalla S. DFT study of the molecular structure, conformational preference, HOMO, LUMO, and vibrational analysis of 2-, and 3-furoyl chloride. Journal of Solution Chemistry. 2017;46(4):741-58.
42. Reed JL. Electronegativity: chemical hardness I. The Journal of Physical Chemistry A. 1997;101(40):7396-400.
43. Arjunan V, Devi L, Subbalakshmi R, Rani T, Mohan S. Synthesis, vibrational, NMR, quantum chemical and structure-activity relation studies of 2-hydroxy-4-methoxyacetophenone. Spectrochimica Acta Part A: Molecular and Biomolecular Spectroscopy. 2014;130:164-77.
44. El-Gammal O, Rakha T, Metwally H, El-Reash GA. Synthesis, characterization, DFT and biological studies of isatinpicolinohydrazone and its Zn (II), Cd (II) and Hg (II)

complexes. Spectrochimica Acta Part A: Molecular and Biomolecular Spectroscopy. 2014;127:144-56.
45. Parr RG, Yang W. Density functional approach to the frontier-electron theory of chemical reactivity. Journal of the American Chemical Society. 1984;106(14):4049-50.
46. Barim E, Akman F. Synthesis, characterization and spectroscopic investigation of N-(2-acetylbenzofuran-3-yl) acrylamide monomer: Molecular structure, HOMO–LUMO study, TD-DFT and MEP analysis. Journal of Molecular Structure. 2019;1195:506-13.
47. Pitzer K. The Nature of the Chemical Bond and the Structure of Molecules and Crystals: An Introduction to Modern Structural Chemistry. Journal of the American Chemical Society. 1960;82(15):4121-.
48. Lipinski CA LF, Dominy BW, Feeney PJ. Experimental and computational approaches to estimate solubility and permeability in drug discovery and development settings. Advanced drug delivery reviews. 2001;46((1-3)):3–26.
49. Husain A, Ahmad A, Khan SA, Asif M, Bhutani R, Al-Abbasi FA. Synthesis, molecular properties, toxicity and biological evaluation of some new substituted imidazolidine derivatives in search of potent anti-inflammatory agents. Saudi Pharmaceutical Journal. 2016;24(1):104-14.
50. Lee S, Lee I, Kim H, Chang G, Chung J, No K. The PreADME Approach: Web-based program for rapid prediction of physico-chemical, drug absorption and drug-like properties. EuroQSAR designing drugs and crop protectants: processes, problems and solutions. 2003:418-20.

HOW TO CITE THIS ARTICLE: Sarkar K, Sarkar S, Das RK. Screening of Some Hamamelitannin Derivatives against *Staphylococcus aureus*: A Computational Perspective. Int. J. Pharm. Sci. Drug Res. 2022;14(6):843-857. **DOI:** 10.25004/IJPSDR.2022.140623